

## Determination of magnetic anisotropy in Fe/Cu multilayers: Equivalence of dynamic and static measurements

Michael J. Pechan

*Department of Physics, Miami University, Oxford, Ohio 45056*

Eric E. Fullerton, W. Robertson,\* and M. Grimsditch

*Materials Science Division, Argonne National Laboratory, Argonne, Illinois 60439*

Ivan K. Schuller

*Physics Department, University of California at San Diego, La Jolla, California 92093-0319*

(Received 3 October 1994; revised manuscript received 11 April 1995)

The magnetic anisotropy of Fe/Cu multilayers has been investigated using dc magnetization, ferromagnetic resonance, and Brillouin light scattering. All three techniques yield equivalent results, which can be attributed to the lack of higher-order terms in the uniaxial anisotropy energies. The intrinsic anisotropy is first-order uniaxial with the easy axis perpendicular to the layers and is interpreted with a simple phenomenological model utilizing a surface anisotropy of  $0.32 \text{ erg/cm}^2$  at each interface.

In recent years there has been considerable interest in the magnetic properties of metallic multilayers.<sup>1</sup> For reasons related to magnetic recording procedures there has been particular interest in the strong perpendicular surface anisotropy observed in some Fe and Co superlattices.<sup>2,3</sup> For sufficiently thin magnetic layers, the intrinsic out-of-plane anisotropy has been observed to be greater than the shape demagnetizing field ( $4\pi M_s$ ) so that the magnetic easy axis is out of the plane. Although the origin of the surface anisotropy has been attributed to the lowered symmetry at the interface<sup>4</sup> other contributions such as magnetocrystalline anisotropy energy involving strain, crystallographic orientation, and electronic effects are also being considered.<sup>5</sup>

Traditional techniques utilized in determining anisotropy include static magnetization (SM) measurements, torque magnetometry, and magneto-dynamic techniques such as Brillouin light scattering (BLS) and ferromagnetic resonance (FMR). Favorable comparison between dynamic techniques (FMR and BLS) has been reported in determining the magnetic anisotropies of Co/Cu superlattices.<sup>6</sup> In addition, comparisons have been made between dynamic and static techniques used in determining interlayer coupling energies in epitaxial trilayer systems.<sup>7</sup> However, significant discrepancies have been reported when comparing dynamic and static techniques in determining interface anisotropy in magnetic multilayers.<sup>8,9</sup> A factor of 5 difference in the magnitude of the interface anisotropy was determined in Mo/Ni superlattices using FMR and SM techniques.<sup>8</sup> Similar differences were observed in Fe/Pd multilayers comparing BLS with SM techniques.<sup>9</sup> These differences have been attributed to higher-order contributions to the anisotropy energy. With this in mind, the present investigation of Fe/Cu superlattices employs both static (SM) and dynamic (BLS and FMR) techniques to carefully evaluate the anisotropy. Our interest in Fe/Cu stems from the magnetization studies which imply that the anisotropy is well described by only a first-order term. In this case, we expect to ob-

tain good agreement between static and dynamic techniques and thereby test the proposed explanation of previous discrepancies. Although the techniques we use have been used extensively to study the anisotropy of thin films and superlattices, we are aware of no direct comparisons of the results obtained by all three techniques. Our present results show good agreement in the determination of the intrinsic anisotropy in Fe/Cu multilayers using FMR, BLS, and SM.

Fe/Cu superlattices with modulation wavelengths ( $\Lambda$ ) ranging from 10 to 300 Å and with equal Fe and Cu thicknesses were prepared by dc magnetron sputtering onto ambient-temperature sapphire and Si substrates. A Cu layer of 500 Å was grown as a base layer on which the superlattice, of total thickness  $\sim 2700$  Å, was deposited. The base pressure was  $(2-4) \times 10^{-7}$  Torr, the Ar pressure during deposition was 2 mTorr, and the sputtering rates were close to 5 Å/sec.

The crystal structure as determined by x-ray diffraction on similar samples has been reported in detail elsewhere.<sup>10</sup>  $M$  vs  $H$  curves, measured using a vibrating-sample magnetometer, yielded the saturation magnetization and static anisotropy energy density. The Brillouin scattering experiments were performed at room temperature using a (5+2)-pass tandem Fabry-Pérot interferometer<sup>11</sup> and a single-mode argon ion laser operating at 514.5 nm. Magnetic fields, ranging from 1 to 6 kG, were applied in the plane of the film and perpendicular to the magnon propagation direction. FMR measurements at 9.2 GHz were made with the applied field in the plane of the film using a standard TE102-mode cavity-based spectrometer.

Figure 1 shows a typical magnetization loop measured on a  $\Lambda=20$  Å Fe/Cu sample for the magnetic field applied parallel and perpendicular to the layers. The Fe volume used in the magnetization calculation is determined utilizing the magnetic layer thickness obtained by x-ray analysis. The room-temperature saturation magnetization  $M_s$ , extracted from the  $M$ - $H$  loops, is shown as

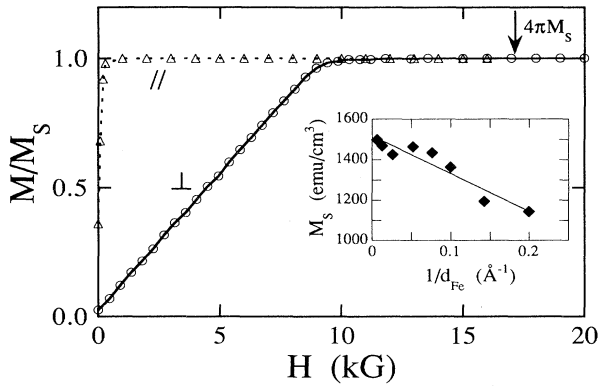


FIG. 1. A room-temperature magnetic hysteresis loop for a  $\Lambda=20 \text{ \AA}$  Fe/Cu multilayer measured parallel and perpendicular to the film. The inset shows the saturation magnetization for equal-layer-thickness Fe/Cu multilayers plotted as a function of the inverse Fe layer thickness. The line is a linear least-squares fit to the data based upon a model described in the text.

an inset in Fig. 1 and varies linearly with  $1/d_{\text{Fe}}$ . Assuming we are measuring the average of a reduced interface magnetization for the first atomic plane and a constant-volume value in the layer interior, one obtains a volume  $M_s$  of  $1520 \text{ emu/cm}^3$  and an interface moment which is reduced 30% relative to the center of the layer. Volume  $M_s$  values lower than that of bulk Fe have been observed in other studies of sputtered Fe/Cu superlattices<sup>12-14</sup> and with Mössbauer studies.<sup>10</sup> The Mössbauer results showed that the two monolayers closest to the interface had a reduced hyperfine field relative to the center of the layer. The hyperfine field at the center of the layer was 315 kOe which is reduced from the bulk value 330 kOe.

Square in-plane  $M$  vs  $H$  hysteresis loops were observed and coercivity values were less than 10 Oe for samples with  $d_{\text{Fe}} > 10 \text{ \AA}$ . For samples with smaller modulation wavelengths there was an increase in both the coercivity and the field required to saturate the in-plane moment. The linear approach to saturation in the perpendicular direction clearly indicates the absence of any higher-order terms in the anisotropy energy. The fact that perpendicular saturation field is much lower than that expected for shape anisotropy alone ( $4\pi M_s = 17 \text{ kG}$ ) indicates an additional uniaxial anisotropy contribution. The area between the parallel and perpendicular loops gives the total anisotropy energy density ( $DM_s/2$ ), where  $D$  is the total effective uniaxial anisotropy field which can be written as a linear combination of the shape anisotropy and the intrinsic anisotropy  $H_a$  according to

$$D = 4\pi M_s - H_a. \quad (1)$$

$H_a > 0$  ( $H_a < 0$ ) implies an easy axis normal to (coincident with) the film plane. For the  $\Lambda=20 \text{ \AA}$  sample shown in Fig. 1, the derived value of  $D$  is 9.0 kG which corresponds to an anisotropy field  $H_a = 8.0 \text{ kG}$ .

Although a general solution of magnetic excitations in layered systems is available in the literature,<sup>15</sup> its staggering complexity (involving more than 10 adjustable pa-

rameters) and the requirement of numerical methods to obtain a solution, make it unattractive for most comparisons with experiment. The other case which has been treated theoretically is the one in which all anisotropy fields (surface and bulk), exchange coupling, and inter-layer coupling are ignored.<sup>16,17</sup> With these approximations it is possible to derive analytical expressions for the magnetic excitations that describe experimental Brillouin scattering results well.<sup>18-20</sup> In the present case the forms of the energy contributions of the shape anisotropy and perpendicular anisotropy fields are identical. It is therefore reasonable to replace the shape anisotropy ( $4\pi M_s$ ) in the expressions from Refs. 16 and 17 by  $D = 4\pi M_s - H_a$ . In the case of infinite wavelength ( $q=0$ ) excitations observed in FMR this approximation can be shown to be rigorously valid.

For a superlattice with equal magnetic and nonmagnetic layer thicknesses, the above considerations lead to the prediction of a band of magnon modes described by<sup>16</sup>

$$\omega = \gamma [H(H+D) + D^2 w/4]^{1/2}, \quad (2)$$

where  $w$  is a parameter which depends on the layer thickness and the magnon wave vector,  $\gamma$  is the gyromagnetic ratio, and  $H$  is the applied magnetic field. In the magnon wave vector  $q=0$  limit, the band collapses to a single frequency given by  $w=0$  so that the FMR frequency is given by

$$\omega = \gamma [H(H+D)]^{1/2}. \quad (3)$$

For nonzero wave vectors and a finite superlattice with  $N$  layers, one expects  $N$  discrete frequencies over the range  $0 \leq w \leq 1$ .<sup>19</sup> The strong feature observed at the top of the band corresponds to  $w=1$  so that the highest feature observed in the Brillouin spectra is given by

$$\omega = \gamma [H + D/2]. \quad (4)$$

Equation (4) corresponds to a surface magnon on a semi-infinite medium. When dealing with a film of finite thickness ( $T$ ), a correction term must be added. Equation (4) takes the form<sup>21</sup>

$$\omega^2 = \gamma^2 [(H + D/2)^2 - (D/2)^2 e^{-2qT}], \quad (5)$$

where  $q$  is the magnon wave vector. In Ref. 16, it has been shown that the surface mode in a superlattice decays only in the magnetic layers; therefore it is reasonable to regard  $T$  as the total magnetic thickness (1350  $\text{\AA}$ ). Equation (5) can then be fitted to the data to determine  $D$ . For  $2qT > 1$  and  $H < D/2$ , Eq. (5) can be recast in a linear form so that the slope  $\gamma_m$  and the intercept frequency  $\omega_0$  are given by

$$\gamma_m = \gamma (1 + \frac{1}{2} e^{-2qT}), \quad \omega_0 = \frac{\gamma^2 D}{2\gamma_m}. \quad (6)$$

Shown in Fig. 2 is a Brillouin spectrum for the same multilayer shown in Fig. 1. The arrow indicates the highest-frequency mode. The measured frequency shifts of the upper mode as a function of applied field are shown as an inset in Fig. 2. A linear fit to the data gives a slope of 3.05 GHz/kG. For our series of samples, the measured slope  $\gamma_m$  ranged from 3.04 to 3.13 GHz/kG,

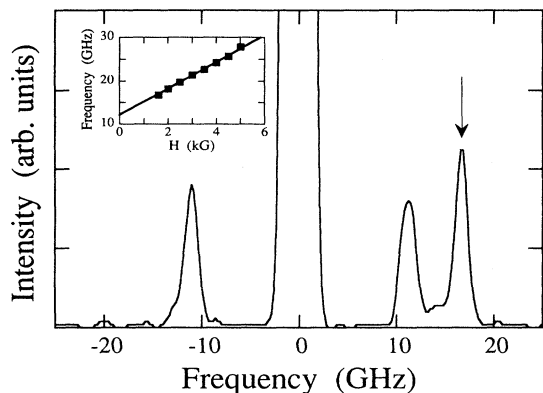


FIG. 2. Brillouin light scattering spectrum for the same  $\Lambda=20$  Å Fe/Cu multilayer shown in Fig. 1 measured in an applied field of 1.6 kG. The arrow indicates the highest-frequency mode. The inset shows the frequency of the high mode versus applied field. The line is a linear least-squares fit to the data based upon a model described in the text. The slope of the line is 3.05 GHz/kG and the intercept 12.1 GHz.

consistent with Eq. (6) and the expected  $\gamma$  value of 2.94 GHz/kG for pure Fe. For the  $\Lambda=20$  Å sample in Fig. 2, the value for  $D$  calculated from Eq. (6) is 8.5 kG as compared with 8.7 kG determined by fitting directly to Eq. (5). These values are in reasonable agreement with the magnetization result of 9.0 kG for the same sample.

Room-temperature FMR spectra were obtained in a parallel field for different  $d_{\text{Fe}}$ . A large absorption was observed, which systematically shifts to higher fields for decreasing modulation, and is taken as the  $q=0$  mode of the system.  $D$  values are extracted using Eq. (3) via the measured value of  $H$  (the applied field where the spectrum crosses background), and the microwave frequency. For the  $\Lambda=20$  Å multilayer, the resonance field is 1 kG, which corresponds to a  $D$  value of 8.6 kG, in close agreement with the BLS result.

Figure 3 shows the value of  $H_a$  determined from Eq.

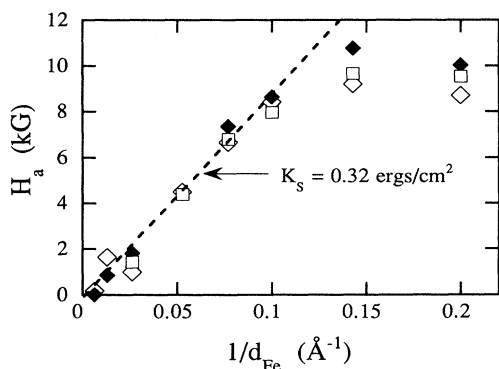


FIG. 3. Intrinsic uniaxial anisotropy field determined by SM (open squares), BLS (closed diamonds), and FMR (open diamonds) plotted as a function of the inverse Fe layer thickness. The dashed line is a linear least-squares fit to the data based upon a model described in the text and indicates an interface anisotropy of 0.32 erg/cm<sup>2</sup>.

(1). The intrinsic anisotropy for all samples measured by all techniques is positive, indicating an easy axis normal to the film plane. In addition, excellent agreement is observed between results obtained from different techniques, validating the assumptions made in analysis of the Brillouin results. The agreement in the Fe/Cu anisotropies obtained with static and dynamic techniques is in contrast to a number of examples in which significantly different anisotropy values were obtained.<sup>8,9</sup> The static technique brings the moment fully to the hard direction, whereas the dynamic techniques (BLS and parallel FMR) merely perturb the moment through small angles about the easy direction. Such small perturbations in a system characterized by both first- and second-order anisotropy energies will not sample the higher-order terms; however a full rotation to the hard direction will measure all terms, resulting in a discrepancy in results obtained. Therefore the present agreement between static and dynamic results can be attributed to the lack of higher-order terms in the uniaxial anisotropy.

The contributions to the intrinsic anisotropy are expected to arise from both volume (crystalline) and interface effects averaged over the magnetic layer. The anisotropy energy density is then commonly written as

$$\frac{H_a M_s}{2} = K_v + \frac{2K_s}{d_{\text{Fe}}}, \quad (7)$$

where  $K_v$  is the crystalline anisotropy and  $2K_s/d_{\text{Fe}}$  is the interface anisotropy treated in the homogeneous magnetization approximation.<sup>22</sup> This simple model predicts the anisotropy will vary linearly with inverse Fe thickness, which is realized in our sample for  $d_{\text{Fe}} \geq 10$  Å. Fitting the linear region in Eq. (7) gives  $K_v$  approximately equal to zero and  $K_s = 0.32 \pm 0.04$  erg/cm<sup>2</sup>. This is in excellent agreement, in both sign and magnitude (0.29 erg/cm<sup>2</sup>), with previous measurements of Fe(110)/Cu multilayers.<sup>23</sup> Measurements on epitaxial Cu/Fe(001)/Au trilayers<sup>24</sup> found the same sign, but larger magnitude (0.62 erg/cm<sup>2</sup>), owing presumably to the different crystallographic orientation and to the exposure of one Fe surface to Au rather than both to Cu.

Equation (7) assumes a purely two-dimensional magnetic interface anisotropy in which the magnetization changes abruptly at the interface. However, as can be seen in Fig. 3, this model breaks down for  $d_{\text{Fe}} < 10$  Å, which most likely results from the finite width of the interface.<sup>10,25,26</sup> A more realistic model would characterize the interface as having an effective interface width which penetrates a distance  $L$  into the film.  $H_a$  would then scale inversely with the Fe thickness down to an Fe thickness of  $2L$  and would then be a constant. For our data, this crossover occurs for the Fe thickness of  $\approx 9$  Å which corresponds to approximately two Fe monolayers at each interface. This result can be compared with the room-temperature Mössbauer results on similarly prepared Fe/Cu multilayers presented in Ref. 10. The Mössbauer hyperfine field distribution for a  $d_{\text{Fe}} = 13$  Å layer could be separated into contributions from the interface which had a reduced hyperfine field relative to the contribution from Fe atoms in the center of the layer. For a  $d_{\text{Fe}} = 6.5$

Å layer, the hyperfine field distribution was characterized by only interface atoms, indicating an effective interface width of two monolayers, in agreement with the magnetization results.

In conclusion, we have examined the anisotropy in a series of sputtered polycrystalline Fe/Cu multilayers by static and dynamic techniques. Interfacial effects, which provide an easy axis normal to the plane of the film, dominate the intrinsic anisotropy; however, owing to shape effects, the overall anisotropy is in plane. The excellent

agreement obtained between static and dynamic techniques is attributed to the lack of higher-order terms in the interface anisotropy.

This work was supported in part by the U.S. Department of Energy, Basic Energy Sciences, Materials Sciences under Contracts No. DE-FG02-86ER45281 (Miami), No. DE-FG03-87ER45332 (UCSD), and No. W31-109-ENG-38 (ANL).

---

\*Present address: National Research Council Canada, Institute for Information Technology, Montreal Road, Building M-50, Ottawa, Canada K1A 0R6.

<sup>1</sup>L. M. Falicov *et al.*, *J. Mater. Res.* **5**, 1299 (1990).

<sup>2</sup>B. N. Engel *et al.*, *Phys. Rev. Lett.* **67**, 1910 (1991).

<sup>3</sup>P. F. Carcia, A. D. Meinhaldt, and A. Suna, *Appl. Phys. Lett.* **47**, 178 (1985).

<sup>4</sup>L. Néel, *J. Phys. Radium* **15**, 225 (1954).

<sup>5</sup>J. G. Gay and R. Richter, *Phys. Rev. Lett.* **56**, 2728 (1986); R. H. Victora and J. M. MacLaren, *J. Appl. Phys.* **73**, 6415 (1993); G. H. O. Daalderop, P. J. Kelley, and F. J. A. den Broeder, *Phys. Rev. Lett.* **68**, 682 (1992); B. N. Engel *et al.*, *Phys. Rev. B* **48**, 9894 (1993); D. Wang, R. Wu, and A. J. Freeman, *Phys. Rev. Lett.* **70**, 869 (1993).

<sup>6</sup>P. Krams *et al.*, *Phys. Rev. Lett.* **69**, 3674 (1992).

<sup>7</sup>J. J. Krebs *et al.*, *Phys. Rev. Lett.* **63**, 1645 (1989); B. Heinrich *et al.*, *Phys. Rev. B* **44**, 9348 (1991); **47**, 5077 (1993).

<sup>8</sup>M. J. Pechan and I. K. Schuller, *Phys. Rev. Lett.* **59**, 132 (1987).

<sup>9</sup>B. Hillebrands *et al.*, *J. Appl. Phys.* **63**, 3880 (1988).

<sup>10</sup>E. E. Fullerton *et al.*, *J. Appl. Phys.* **73**, 7370 (1993).

<sup>11</sup>J. R. Sandercock, in *Light Scattering in Solids III*, edited by M. Cardona and G. Güntherodt (Springer, Berlin, 1982).

<sup>12</sup>H. M. van Noort, F. J. A. den Broeder, and H. J. G. Draaisma, *J. Magn. Magn. Mater.* **51**, 273 (1985).

<sup>13</sup>H. J. G. Draaisma, H. M. van Noort, and F. J. A. den Broeder, *Thin Solid Films* **126**, 117 (1985).

<sup>14</sup>S. B. Qadri *et al.*, *J. Vac. Sci. Technol. A* **9**, 430 (1991).

<sup>15</sup>B. Hillebrands, *Phys. Rev. B* **41**, 530 (1990).

<sup>16</sup>R. E. Camley, T. S. Rahman, and D. L. Mills, *Phys. Rev. B* **27**, 261 (1983).

<sup>17</sup>P. Grünberg and K. Mika, *Phys. Rev. B* **27**, 2955 (1983).

<sup>18</sup>M. Grimsditch *et al.*, *Phys. Rev. Lett.* **51**, 498 (1983); A. Kueny *et al.*, *Phys. Rev. B* **29**, 2878 (1984).

<sup>19</sup>B. Hillebrands *et al.*, *Phys. Rev. B* **34**, 9000 (1986).

<sup>20</sup>B. Hillebrands and G. Güntherodt, *J. Appl. Phys.* **61**, 3756 (1987).

<sup>21</sup>K. W. Damon and J. R. Eshbach, *J. Phys. Chem. Solids* **19**, 308 (1961).

<sup>22</sup>U. Gradmann, *J. Magn. Magn. Mater.* **54–57**, 733 (1986).

<sup>23</sup>L. Smardz *et al.*, *J. Magn. Magn. Mater.* **104–107**, 1885 (1992).

<sup>24</sup>B. Heinrich *et al.*, *J. Appl. Phys.* **70**, 5769 (1991).

<sup>25</sup>M. J. Pechan, *J. Appl. Phys.* **64**, 5754 (1988).

<sup>26</sup>E. E. Fullerton *et al.*, *Phys. Rev. B* **45**, 9292 (1992).